A mixing ratios-based formulation for multicomponent reactive transport

M. De Simoni,[1,2] X. Sanchez-Vila,[3] J. Carrera,[4] and M. W. Saaltink[3]

Received 19 June 2006; revised 7 March 2007; accepted 26 March 2007; published 13 July 2007.

[1] Chemical reactions are driven by disequilibrium, which is often caused by mixing. Therefore quantification of the mixing rate is essential for evaluating the fate of solutes in natural systems, such as rivers, lakes, and aquifers. We propose a novel mixing ratios-based formulation to evaluate solute concentrations and reaction rates when equilibrium aqueous reactions and precipitation/dissolution of minerals are driven by mixing of different end-members. Each end-member corresponds to a water from a given source with a specific chemical signature. The approach decouples the solute transport and chemical speciation problems, so that mixing ratios can be first obtained from the solution of conservative transport and then be used in general speciation codes to obtain the concentration of reacting species. One key finding is a general expression for reaction rates which demonstrates that the amount of reactants evolving into products depends on the rate at which solutions mix. Our formulation constitutes a general framework according to which one can design and interpret experimental analyses devoted to study mixing-driven reactive processes and obtain transverse dispersion coefficients. The formulation is also proposed as a useful tool to derive analytical solutions of reactive transport problems and may result computationally advantageous when compared to previous approaches to reactive transport modeling. We apply the developed formulation to provide an analytical solution of the reactive transport process resulting from mixing different $CaCO_3$-saturated waters in a two-dimensional setup.

Citation: De Simoni, M., X. Sanchez-Vila, J. Carrera, and M. W. Saaltink (2007), A mixing ratios-based formulation for multicomponent reactive transport, *Water Resour. Res.*, *43*, W07419, doi:10.1029/2006WR005256.

1. Introduction

[2] The relevance of mixing in reactive transport phenomena is well documented; mixing controls chemical speciation in aquatic systems [*Witters*, 1998; *Aucour et al.*, 2003] and has a significant impact in pollutant concentrations where surface and subsurface waters interact [*Choi et al.*, 1998; *Tonkin et al.*, 2002; *Balistrieri et al.*, 2003]. Moreover, mixing of waters originally in equilibrium with a mineral drives precipitation and dissolution of mineral species [*Rezaei et al.*, 2005; *Emmanuel and Berkowitz*, 2005]. Because of their complexity and extension, special attention has been given to mixing-driven processes governing the geochemistry of carbonate systems [e.g., *Sanford and Konikow*, 1989; *Corbella et al.*, 2003; *Singurindy et al.*, 2004; *Rezaei et al.*, 2005; *Romanov and Dreybrodt*, 2006], including karst development [*Gabrovšek and Dreybrodt*, 2000; *Kaufmann*, 2003]. Mixing may also be the governing process for microbial reactions [*Nambi et al.*, 2003; *Chu et al.*, 2005; *Knutson et al.*, 2005], which are relevant in natural attenuation problems [*Cirpka et al.*, 1999]. Hence it is not surprising that emphasis has been placed in characterizing mixing [*Gramling et al.*, 2002; *Jose and Cirpka*, 2004].

[3] Mixing can be characterized in terms of mixing ratios, which are defined as the proportion of each of the mixing waters in the mixed sample. The original mixing waters, from which all mixtures are derived, are often called end-members. Presumably, end-members differ in the concentrations of some species (that is, they display different "chemical signatures"). The concentration of a conservative solute in a mixture is obtained by linear combination of the concentrations of the end-members. Mixing ratios are useful because they can be quantified from the analysis of conservative chemical species even when end-members are uncertain [*Carrera et al.*, 2004; *Rueedi et al.*, 2005]. Deviations from perfect mixing may be used to identify the chemical processes controlling the system [*Tonkin et al.*, 2002; *Aucour et al.*, 2003] or to determine parameters characterizing plume transport [*Cirpka et al.*, 2006].

[4] Formulations of mixing-driven chemical processes are complex. Some of these can be eliminated using equilibrium relations, according to the phase rule. For example, carbonate systems are typically governed by six aqueous species (H^+, OH^-, Ca^{2+}, HCO_3^-, CO_3^{2-}, $CO_{2(aq)}$) and four reactions (water, HCO_3^- and CO_3^{2-} dissociation, and calcite dissolution), plus two constant activity species (H_2O and $CaCO_3$). So the system has two degrees of freedom [e.g., *Rezaei et al.*, 2005]. Yet, *Sanford and Konikow* [1989]

[1]Dipartimento di Ingegneria Idraulica, Ambientale, Infrastrutture Viarie, Rilevamento, Politecnico di Milano, Milan, Italy.
[2]Now at ENI, E and P division, Via Emilia 1, 20097 San Donato Milanese, Italy.
[3]Department of Geotechnical Engineering and Geosciences, Technical University of Catalonia, Barcelona, Spain.
[4]Institut de Ciències de la Terra Jaume Almera, CSIC, Barcelona, Spain.

0043-1397/07/2006WR005256

correctly solved the problem using one independent variable. We attribute this paradox to the fact that their problem was driven by mixing, so that the proportion of one of the end-members (i.e., the mixing ratio) was the only independent variable. The question is, thus, whether reactive transport problems can be formulated in terms of mixing ratios.

[5] The objective of this paper is to present a novel mixing ratios-based formulation to solve reactive transport problems in the case of equilibrium aqueous reactions and precipitation/dissolution of minerals induced by mixing of different solutions. The work extends that of *De Simoni et al.* [2005], who solved multispecies reactive transport using components and assuming chemical equilibrium. As such, it does not apply to cases where reactions need to be treated kinetically (that is, their characteristic reaction time is long compared to diffusive mixing characteristic times) nor to reactions where immobile species display variable activity (for example, coprecipitation, solid mixtures, or ion exchange reactions).

2. Theoretical Developments

[6] Modeling reactive transport involves two coupled ingredients, mass balances of species and a set of equations describing reactions among species.

2.1. Species Transport Equations

[7] Species mass balance can be written [e.g., *Saaltink et al.*, 1998; *Molins et al.*, 2004] as

$$\frac{\partial(\mathbf{m})}{\partial t} = \mathbf{M}L(\mathbf{c}) + \mathbf{f}. \tag{1}$$

Here vector $\mathbf{m}$ contains the mass of species per unit volume of medium, and vector $\mathbf{c}$ contains species concentrations ($\mathbf{m} = n\mathbf{c}$ for mobile species in a medium of porosity n; $n = 1$ for single phase). Matrix $\mathbf{M}$ is diagonal, and its diagonal terms are unity when a species is mobile and 0 otherwise; $\mathbf{f}$ is a source/sink term, which is used to represent chemical reactions. The linear operator $L(\mathbf{c})$ in equation (1) is defined as $L(\mathbf{c}) = -\nabla \cdot (n\mathbf{v}\mathbf{c}) + \nabla \cdot (n\mathbf{D}\nabla\mathbf{c})$, where $\mathbf{D}$ is the dispersion tensor and $\mathbf{v}$ is the fluid velocity (we assume that $\mathbf{D}$ and $\mathbf{v}$ are the same for all species).

2.2. Equilibrium Reactions

[8] Chemical reactions can be assumed at equilibrium when their rate is fast compared to transport processes. Under these conditions, $\mathbf{f} = \mathbf{S}_e^T\mathbf{r}$, where $\mathbf{r}$ is the vector of reaction rates (expressed per unit volume of medium) and $\mathbf{S}_e$ is the stoichiometric matrix of the chemical system ($\mathbf{S}_e$ is an $N_r \times N_s$ matrix, N_r and N_s being the number of reactions and of chemical species, respectively) [see, e.g., *Saaltink et al.*, 1998].

[9] Equilibrium is described by the mass action law, which can be written as $\mathbf{S}_e \log \mathbf{a} = \log \mathbf{K}$, where $\mathbf{K}$ is the vector of chemical equilibrium constants and $\mathbf{a}$ is the vector of species activities. Some species (here called constant activity species), such as water and minerals, can be assumed as having unit activity.

[10] The mass action law can be written such that the activities of N_r secondary species can be calculated from the activities of $N_s - N_r$ primary species [*Steefel and Mac Quarrie*, 1996; *Saaltink et al.*, 1998]. We choose as primary species the N_c constant activity species plus $N_s - N_r - N_c$ aqueous species. Since we consider mineral species to have constant activities, all secondary species are aqueous. We split vector $\mathbf{a}$ as $\mathbf{a} = (\mathbf{a}_c\ \mathbf{a}_a'\ \mathbf{a}_a'')$, where $\mathbf{a}_c$ contains the activities of the N_c constant activity species, $\mathbf{a}_a'$ contains the N_u ($= N_s - N_r - N_c$) activities of aqueous primary species, and $\mathbf{a}_a''$ is composed by the N_r activities of secondary species. Likewise, we subdivide $\mathbf{S}_e$ into three parts. It is always possible to redefine the chemical system so that the contribution of the secondary species to $\mathbf{S}_e$ is minus the identity matrix $\mathbf{I}$. That is, the $\mathbf{S}_e$ matrix is decomposed as $\mathbf{S}_e = (\mathbf{S}_{ec}|\mathbf{S}_{ea}'| - \mathbf{I})$, where $\mathbf{S}_{ec}$ and $\mathbf{S}_{ea}'$ correspond to the stoichiometric coefficients of constant activity and primary species, respectively. This allows an explicit calculation of the secondary species activities from mass action laws as

$$\log \mathbf{a}_a'' = \mathbf{S}_{ea}' \log \mathbf{a}_a' - \log \mathbf{K}. \tag{2}$$

Alternatively, equation (2) can be written in terms of concentrations ($\mathbf{c} = (\mathbf{c}_c\ \mathbf{c}_a)^T = (\mathbf{c}_c\ \mathbf{c}_a'\ \mathbf{c}_a'')^T$; that is, $\mathbf{c}_a'$ and $\mathbf{c}_a''$ represent concentrations of primary and secondary species, respectively) as

$$\log \mathbf{c}_a'' = \mathbf{S}_{ea}' \log \mathbf{c}_a' - \log \mathbf{K}^*, \tag{3}$$

where $\mathbf{K}^*$ is a vector of equivalent equilibrium constants defined as:

$$\log \mathbf{K}^* = \log \mathbf{K} - \left(\mathbf{S}_{ea}'|-\mathbf{I}\right) \log \gamma_a, \tag{4}$$

γ_a being the vector of activity coefficients.

[11] A reactive transport process is fully described once concentrations of the N_s species are obtained, together with the N_r reactions rates ($N_s + N_r$ unknowns). This requires solving the coupled N_s mass balance equations [equation (1)] and N_r equilibrium equations [equation (3)].

2.3. Components

[12] Solution of reactive transport problems can be simplified upon defining components [*Lichtner*, 1985; *Steefel and Mac Quarrie*, 1996; *Saaltink et al.*, 1998; *Molins et al.*, 2004; *De Simoni et al.*, 2005] by introducing an auxiliary component matrix, $\mathbf{U}$. Among the different possible definitions for matrix $\mathbf{U}$, we chose to define it so that $\mathbf{U}\mathbf{S}_e^T = (\mathbf{S}_{ec}\ \mathbf{0})^T$. Since $\mathbf{S}_e = (\mathbf{S}_{ec}|\mathbf{S}_{ea}'| - \mathbf{I})$, an expression for $\mathbf{U}$ is

$$\mathbf{U} = \begin{pmatrix} \mathbf{U}_c \\ \mathbf{U}_a \end{pmatrix} = \begin{pmatrix} \overset{N_c}{\leftrightarrow} & \overset{N_u}{\leftrightarrow} & \overset{N_r}{\leftrightarrow} \\ \mathbf{I} & \mathbf{0} & \mathbf{0} \\ \mathbf{0} & \mathbf{I} & \mathbf{S}_{ea}'^T \end{pmatrix} \begin{matrix} \updownarrow N_c \\ \updownarrow N_u \end{matrix} \tag{5}$$

Multiplication of equation (1) by $\mathbf{U}$ leads to

$$\frac{\partial(\mathbf{m}_c)}{\partial t} = \mathbf{M}_c L_t(\mathbf{m}_c) + \mathbf{S}_{ec}^T\mathbf{r}, \tag{6}$$

$$\frac{\partial(n\mathbf{u})}{\partial t} = L_t(\mathbf{u}) \tag{7}$$

where vector $\mathbf{m}_c$ contains the mass of constant activity species and $\mathbf{u}$ is a vector of N_u (aqueous) components defined as

$$\mathbf{u} = \mathbf{U}_a\mathbf{c} = \mathbf{c}'_a + \left(\mathbf{S}'_{ea}\right)^T\mathbf{c}''_a. \quad (8)$$

[13] Equation (7) represents N_u transport equations without reaction sink/source terms. That is, components are indeed conservative quantities in systems at equilibrium. Vector $\mathbf{u}$ contains only aqueous species so that we can leave out matrix $\mathbf{M}$ in equation (7), while $\mathbf{M}_c$ [equation (6)] is the part of $\mathbf{M}$ referring to constant activity species.

[14] Once equation (7) is solved (with appropriate boundary and initial conditions), (aqueous) solutes concentrations are obtained from the expression of $\mathbf{u}$ in terms of concentrations species [equation (8)] and the mass action law [equation (3)]. Equilibrium reaction rates are then defined from transport equations [equation (1)] of secondary species [*De Simoni et al.*, 2005] as:

$$\mathbf{r} = L\left(\mathbf{c}''_a\right) - \frac{\partial\left(n\mathbf{c}''_a\right)}{\partial t}. \quad (9)$$

The mass evolution of the constant activity species is finally obtained upon substituting $\mathbf{r}$ into equation (6).

[15] Here we focus on reactive transport problems induced by mixing. We define mixing ratio, α_i, as the proportion of end-member i in a water sample. Thus, the concentration of a conservative species can be written in terms of the mixing ratios and the concentrations of the end-members as:

$$c = \sum_{i=1}^{N_i} \alpha_i c_i, \quad (10)$$

where c is the concentration of the water sample and c_i the concentration of a conservative species for end-member i. In equation (10), N_i is the number of end-members, which is equal to the number of mixing ratios defining the problem. Actually the number of independent variables that could be used to fully define the system is equal to $N_i - 1$, since the α_i values should satisfy $\sum_{i=1}^{N_i} \alpha_i = 1$.

[16] From equation (10), it turns out that the mixing ratios are conservative quantities, and thus it is possible to define the transport problem as a suite of transport equations for the different mixing ratios. This constitutes the starting point of our mixing ratios-based formulation.

3. Solution Methodology

[17] The methodology to evaluate solute concentrations and reaction rates in mixing-driven reactive transport processes is developed over four steps.

3.1. Step (1) Evaluation of the Mixing Ratios

[18] As explained in the previous section, the independent mixing ratios α_i ($i = 1, N_i - 1$) satisfy conservative transport equations

$$\frac{\partial \alpha_i}{\partial t} = L(\alpha_i), \quad (11)$$

with homogeneous boundary and initial conditions, except where end-member i is initially present or enters the system. Equation (11) can be solved using analytical techniques or numerical tools to provide mixing ratios at any location and time. Mixing ratios can also be mapped from chemical analyses at locations where water is sampled [*Carrera et al.*, 2004] without the need for solving equation (11).

3.2. Step (2) Evaluation of Components

[19] Components are defined by means of equation (8); being conservative quantities, they are linearly related to α_i

$$\mathbf{u} = \sum_i \alpha_i \mathbf{u}_i, \quad (12)$$

where $\mathbf{u}_i$ is the vector of components concentrations in the ith end-member. Equation (12) can also be obtained directly from equations (8) and (10).

3.3. Step (3) Speciation Calculations

[20] Once system components have been evaluated, $\mathbf{c}_a$(= $(\mathbf{c}'_a\ \mathbf{c}''_a)^T$) is obtained from the nonlinear algebraic system of equations (3) and (8). Vector $\mathbf{c}_a$ may depend on several factors, including pH, salinity, and temperature. This generally leads to nonlinear functional dependences on mixing ratios. Thus, speciation may be computationally demanding; yet it is a standard option on speciation codes, such as PHREEQC [*Parkhurst*, 1995]. Speciation calculations can be done for a prespecified set of mixing ratios (for example, considering two end-members, one could compute the solution for α_i ranging between 0 and 1 with an appropriate step). Then, in conjunction with solutions of step (1), these calculations would provide the spatial and temporal distribution of $\mathbf{c}_a$. Thus, there is no need to solve the system of equations (3) and (8) at all domain nodes for every time step and the computational efficiency in speciation calculations may increase.

3.4. Step (4) Calculation of Reaction Rates

[21] Speciation provides the concentrations of primary and secondary species as a (nonlinear) function of mixing ratios. Substituting $\mathbf{c}''_a = \mathbf{c}''_a(\alpha_i)$ into equation (9), and after some algebra, leads to [*De Simoni et al.*, 2005]:

$$\mathbf{r} = n\sum_i \frac{\partial^2 \mathbf{c}''_a}{\partial \alpha_i^2}\left(\nabla^T \alpha_i \mathbf{D} \nabla \alpha_i\right). \quad (13)$$

[22] This is a key result in our analysis and highlights that reaction rates are given by the sum of the individual contributions which themselves are the product of two terms. The first one reflects the nonlinearity in the speciation (notice that a linear variation of $\mathbf{c}''_a$ with α_i would lead to a null second derivative). The second term is the contribution due to transport and is always positive; hence the sign of the reaction rate is governed by the first term. Once $\mathbf{r}$ is computed, $\mathbf{m}_c$ can be obtained from equation (6).

[23] Evaluation of reaction rates may be further simplified. The term $(\nabla^T \alpha_i \mathbf{D} \nabla \alpha_i)$ in equation (13) is known once the mixing ratio is evaluated (step (1)). Several alternatives are available to provide the first term on the right-hand side of equation (13). In relatively simple cases, $\partial^2 c''_{am} / \partial \alpha_i^2$ (c''_{am} represents the mth secondary species) may be evaluated analytically or numerically (for instance by means of a MATLAB procedure, as we do for the example provided in

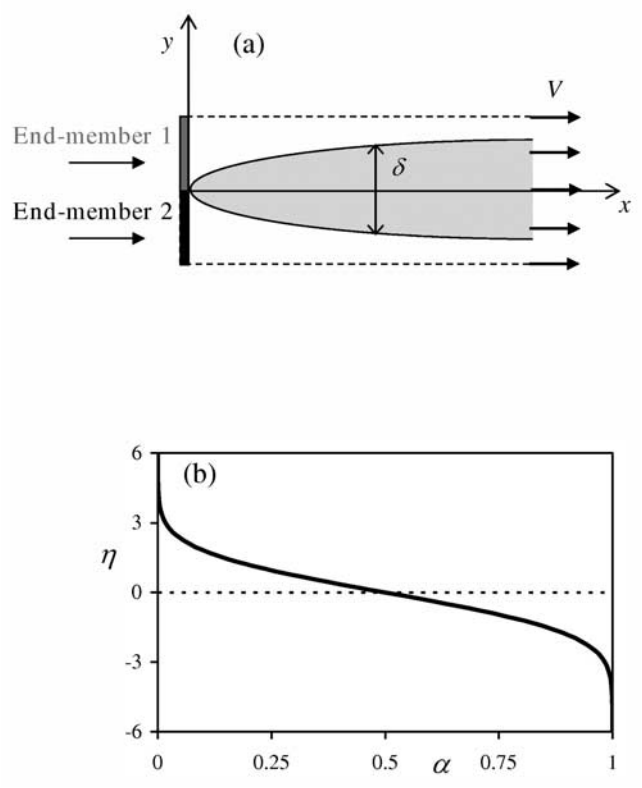

Figure 1. (a) Sketch of the domain; δ represents the extension of the mixing zone; (b) Dependence of α on the normalized transverse coordinate η. The plot is representative of any section transverse to flow (x = constant).

section 4). Alternatively, one could (a) plot c_{am}'' versus α_i (these kinds of plots can be obtained, for example, using codes such as PHREEQC), (b) interpolate the obtained plot by means of a high order polynomial, and (c) take the second derivative of the interpolating function. This methodology is similar to that presented by *Romanov and Dreybrodt* [2006] to compute the derivatives of the concentration in equilibrium with respect to salinity in a freshwater-saline water mixing problem.

4. Illustrative Example

[24] We consider a two-dimensional homogeneous domain under uniform flow conditions. The velocity, V, is aligned along the x axis (Figure 1a). Mixing is controlled by a uniform dispersion tensor D_L and D_T being the longitudinal and transverse components, respectively. Two end-members enter the domain at $x = 0$, creating a mixing zone of transverse extent δ (Figure 1a).

[25] A large number of environmental problems can be modeled by means of this scheme, mixing of freshwater and seawater in coastal aquifers [*Rezaei et al.*, 2005; *Romanov and Dreybrodt*, 2006], hydrochemistry at river confluences [*Aucour et al.*, 2003], or processes of river water infiltrating in aquifers [*Balistrieri et al.*, 2003]. It can also depict the mixing of two parallel streams, respectively, containing an electron acceptor and donor when modeling growth of dechlorinating microorganisms [*Nambi et al.*, 2003; *Chu et al.*, 2005].

[26] This scheme may be helpful in designing/interpreting field or laboratory experiments to analyze chemical reactions in mixing zones [*Singurindy et al.*, 2004]. A relevant quantity in defining the setup for these experiments is the extent, δ, of the mixing zone. Inside this zone, dispersive and advective time-scales are of the same order of magnitude, that is $\delta^2 / D_T \approx x / V$, thus revealing that δ increases with $\sqrt{x}$ [*Nambi et al.*, 2003; *Chu et al.*, 2005] and also with $\sqrt{D_T}$ [*Rezaei et al.*, 2005].

[27] We apply our proposed formulation to analytically solve the process arising from the mixing of two $CaCO_3$-saturated end-members under chemical equilibrium conditions. The two end-members have different chemistry composition but are both saturated with respect to calcite. We exclude the possibility of complete mineral dissolution, so that equilibrium with respect to calcite is assumed in the whole domain at all times. In addition to steady state flow, we assume pseudo-steady state transport; that is, aqueous concentrations do not change with time even though minerals do. This geochemical setup is frequently employed to analyze the evolution of calcite dissolution/precipitation in coastal aquifers [e.g., *Sanford and Konikow*, 1989; *Singurindy et al.*, 2004].

[28] The chemical system is described by four chemical reactions. These reactions are written putting on evidence aqueous primary and secondary species. Among the different possibilities available to select these species, we chose $CO_{2(aq)}$ and H^+ as aqueous primary species. Thus,

$$\text{R1} \qquad HCO_3^- = CO_{2(aq)} + H_2O - H^+ \tag{14a}$$

$$\text{R2} \qquad CO_3^{2-} = CO_{2(aq)} + H_2O - 2H^+ \tag{14b}$$

$$\text{R3} \qquad Ca^{2+} = CaCO_3 - CO_{2(aq)} - H_2O + 2H^+ \tag{14c}$$

$$\text{R4} \qquad OH^- = H_2O - H^+ \tag{14d}$$

We identify $CaCO_3$ and H_2O as constant activity species, while Ca^{2+}, HCO_3^-, CO_3^{2-}, and OH^- are secondary species, thus

$$\begin{aligned}\mathbf{c} &= \left(\mathbf{c}_c \quad \mathbf{c}_a' \quad \mathbf{c}_a''\right)^T \\ &= \left(CaCO_3 \quad H_2O \middle| CO_{2(aq)} \quad H^+ \middle| HCO_3^- \quad CO_3^{2-} \quad Ca^{2+} \quad OH^-\right)^T\end{aligned} \tag{15}$$

The ensuing stoichiometric matrix of the reactions R1–R4 [equations (14a)–(14d)] is

$$\mathbf{S}_e = \left(\begin{array}{cc|cc|cccc} CaCO_3 & H_2O & CO_2 & H^+ & HCO_3^- & CO_3^{2-} & Ca^{2+} & OH^- \\ 0 & 1 & 1 & -1 & -1 & 0 & 0 & 0 \\ 0 & 1 & 1 & -2 & 0 & -1 & 0 & 0 \\ 1 & -1 & -1 & 2 & 0 & 0 & -1 & 0 \\ 0 & 1 & 0 & -1 & 0 & 0 & 0 & -1 \end{array}\right) = \left(\mathbf{S}_{ec} \middle| \mathbf{S}_{ea}' \middle| -\mathbf{I}\right) \tag{16}$$

Hence the source term in the species mass balance [equation (1)] is

$$\mathbf{f} = (\mathbf{S}_e)^T \mathbf{r} = \begin{pmatrix} r_3; & r_1 + r_2 - r_3 + r_4; & r_1 + r_2 - r_3; \\ r_1 - 2r_2 + 2r_3 - r_4; & -r_1; & -r_2; \quad -r_3; \quad -r_4 \end{pmatrix}^T \tag{17}$$

and vector $\mathbf{K}^* = (K_1^* K_2^* K_3^* K_4^*)^T$ [equation (4)] reads

$$\mathbf{K}^* = \left(\frac{K_1 \gamma_{HCO_3^-} \gamma_{H^+}}{\gamma_{CO_2}}; \frac{K_2 \gamma_{H^+}^2 \gamma_{CO_3^{2-}}}{\gamma_{CO_2}}; \frac{K_3 \gamma_{Ca^{2+}} \gamma_{CO_2}}{\gamma_{H^+}^2}; K_4 \gamma_{OH} \gamma_H \right)^T \tag{18}$$

Here K_1, K_2, K_3, and K_4 are the equilibrium constants of reactions R1–R4 [equations (14a)–(14d)], ($K_1 = 10^{6.3447}$; $K_2 = 10^{16.6735}$; $K_3 = 10^{-8.1934}$; $K_4 = 10^{13.9951}$); while γ_m is the activity coefficient of species m.

[29] The two end-members (Figure 1a) contain the six aqueous constituents [equation (15)] at different concentrations; they can also contain solutes which do not contribute directly to the carbonate system, such as Na^+ and Cl^- that may control water salinity. Since solutions may be not diluted, we model γ_m using the extended Debye-Hückel equation:

$$\log \gamma_m = \frac{A z_m^2 \sqrt{I_s}}{1 + B \mathring{a}_m \sqrt{I_s}} + \mathring{b} I_s \tag{19}$$

where I_s is the ionic strength, defined as $I_s = 0.5 \sum_{m=1}^{N_s} c_{am} z_m^2$ [*Helgerson and Kirkham*, 1974]; z_m and $\mathring{a}_m$ are the valence and the ionic radius of species m, respectively; $\mathring{b}$ is a characteristic constant; A and B are temperature dependent parameters. We set $A = 0.5092$, $B = 0.3282$ (values at 25°C), $\mathring{b} = 0.041$. Values of $\mathring{a}_m$ are provided in Table 1.

[30] Assuming that I_s is dominated by nonreactive species (such as Na^+ and Cl^-), the ionic strength of a mixture of two waters is $I_s = \alpha(I_{s,1} - I_{s,2}) + I_{s,2}$, where subscripts 1 and 2 refer to the two end-members and α is the mixing ratio, which corresponds in this case to the contribution of end-member 2 (thus the fraction of end-member 1 is 1-α). This assumption, which basically implies assuming that precipitation or dissolution of calcite does not change the ionic strength, simplifies the mathematical problem. Indeed, the dependence of I_s on species, such as calcium and bicarbonate, would bring $\mathbf{K}^*$ to depend on these species concentrations and thus would lead an additional nonlinearity to the problem.

[31] We apply the methodology outlined in section 3 to obtain the spatial and temporal distribution of species concentration and reaction rates.

4.1. Step (1) Evaluation of the Mixing Ratios

[32] We consider an advective-dominated transport problem, characterized by a large Peclet number, $Pe = Vx / D_T$. In steady state and neglecting longitudinal dispersion [*Rezaei et al.*, 2005], equation (11) becomes $-V\frac{\partial \alpha}{\partial x} + D_T \frac{\partial^2 \alpha}{\partial y^2} = 0$. The domain of the problem is ($x \in [0, +\infty]$; $y \in [-\infty, +\infty]$), and the mixing ratio is prescribed along the boundary as $\alpha(x = 0, y \in [0, \infty]) = 0, \alpha(x = 0, y \in [0, -\infty]) = 1$. The mathematical solution of this problem is [e.g., *Haberman*, 1998, p. 449]

$$\alpha = \frac{1}{2}\left(1 - erf\left[\frac{\eta}{2}\right]\right), \tag{20}$$

where $\eta = \sqrt{Pe}\, y / x$ is a similarity variable, representing a normalized transverse coordinate and $erf[\cdot]$ is the error function.

[33] The dependence of mixing ratios on η is illustrated in Figure 1b. Since α depends solely on η [equation (20)], Figure 1b is representative of a generic section transverse to flow (x = constant).

4.2. Step (2) Evaluation of Components

[34] Using equation (5) for $\mathbf{U}$ and equation (16) for $\mathbf{S}_e$, we obtain two components

$$\mathbf{u} = \begin{pmatrix} c_{CO_2} + c_{HCO_3^-} + c_{CO_3^{2-}} - c_{Ca^{2+}} \\ c_{H^+} - c_{HCO_3^-} - 2c_{CO_3^{2-}} + 2c_{Ca^{2+}} - c_{OH^-} \end{pmatrix} = \begin{pmatrix} u_I \\ u_{II} \end{pmatrix} \tag{21}$$

where u_I is the initial total dissolved carbon minus calcium, and u_{II} is the total charge, which are indeed conservative quantities [*Andre and Rajaram*, 2005]. Since α is already known [equation (20)], $\mathbf{u}(x, y)$ (actually $\mathbf{u}(\eta)$) may be evaluated using equation (12).

4.3. Step (3) Speciation Calculations

[35] Once $\mathbf{u}$ is given, aqueous species concentrations are the solution of the nonlinear algebraic system provided by equations (3) and (21). We first calculate $\mathbf{c}_a'$; using the mass action laws [equations (3)] to eliminate secondary species from equation (21) leads to a sixth order polynomial for c_{H^+}:

$$\begin{aligned} &c_{H^+}^6 \left(4K_3^* - 1\right) + c_{H^+}^5 \left[2(u_I + u_{II}) - K_1^* + 4K_1^* K_3^*\right] \\ &+ c_{H^+}^4 \left[-2u_{II}(2u_I + u_{II}) + K_1^*(3u_I + 2u_{II}) + 2K_4^* - K_2^* + K_1^{*2} K_3^*\right] \\ &+ c_{H^+}^3 \left[-K_1^*(u_I + u_{II})(2u_I + u_{II}) - 2(2u_I + u_{II})K_4^* + 2K_4^* K_1^* + 2K_2^*(2u_I + u_{II})\right] \\ &+ c_{H^+}^2 \left[-K_1^* K_4^*(3u_I + 2u_{II}) - K_4^{*2} - K_2^*(2u_I + u_{II})^2 + 2K_2^* K_4^*\right] \\ &+ c_{H^+} \left[-2K_2^* K_4^*(2u_I + u_{II}) - K_1 K_4^{*2}\right] - K_2^* K_4^{*2} = 0 \end{aligned} \tag{22a}$$

The concentration of the primary species $CO_{2(aq)}$ is

$$c_{CO_2} = \frac{-c_{H^+}^2 + c_{H^+}(2u_I + u_{II}) + K_4^*}{2c_{H^+} + K_1^*} \tag{22b}$$

Given $\mathbf{c}_a'$, concentrations of secondary species are provided by equation (3). From a practical point of view, c_{H^+} and c_{CO_2} are calculated solving (numerically) equation (22a) and

Table 1. Ionic Radius, $\mathring{a}_m$, of the System Species

Species	H^+	OH^-	Ca^{2+}	HCO_3^-	CO_3^{2-}	$CO_{2(aq)}$
$\mathring{a}_m$	9.0	3.0	6.0	4.0	5.0	3.0

substituting the solution in equation (22b), under the constraint that both concentrations have to be real and positive.

4.4. Step (4) Calculation of Reaction Rates

[36] Using equation (13), the reaction rates result

$$\mathbf{r} = \frac{nV}{x}\frac{\partial^2 \mathbf{c}_a''}{\partial \alpha^2}\left(\frac{d\alpha}{d\eta}\right)^2, \tag{23}$$

where $d\alpha / d\eta = -1/(2\sqrt{\pi})\exp[-\eta^2/4]$. Substituting in equation (3) $\mathbf{c}_a'$ as function of $\mathbf{u}(\alpha)$ and $\mathbf{K}^*(I(\alpha))$ allows defining the functional dependence $\mathbf{c}_a'' = \mathbf{c}_a''(\alpha)$, then an ad hoc code can be employed to evaluate $\partial^2 \mathbf{c}_a'' / \partial \alpha^2$ and quantify $\mathbf{r}$ by means of equation (23). Equation (3) reveals that every $\mathbf{c}_{am}''$ depends on α through $\mathbf{c}_a'$ and $\mathbf{K}_m^*$. Thus, we can set $\mathbf{c}_{am}'' = w(\mathbf{c}_a')g(\mathbf{K}_m^*)$ ($w(\cdot)$ and $g(\cdot)$ being functions specified by mass action laws) and separate three contributions in $\partial^2 \mathbf{c}_{am}'' / \partial \alpha^2$:

$$\frac{\partial^2 c_{am}''}{\partial \alpha^2} = g\left(K_m^*\right)\frac{\partial^2 w(\mathbf{c}_a')}{\partial \alpha^2} + 2\frac{\partial w(\mathbf{c}_a')}{\partial \alpha}\frac{\partial g\left(K_m^*\right)}{\partial \alpha} + w(\mathbf{c}_a')\frac{\partial^2 g\left(K_m^*\right)}{\partial \alpha^2}. \tag{24}$$

[37] The first term on the right-hand side of equation (24) is related to primary species variations and is typically referred to as algebraic effect [*Corbella et al.*, 2003; *Molins et al.*, 2004]. The last term contributes to reaction rates when the end-members have different ionic strength, for example, in the presence of different salinity. The middle term in the right-hand side of equation (24) is a cross term, which vanishes in the absence of either algebraic or ionic strength effects.

[38] At this stage, the system is fully solved, and we use the solution to simulate dissolution and precipitation of calcite because of the mixing of two $CaCO_3$-saturated waters inside the fresh-saltwater mixing zone of coastal aquifers. We recall that the derived analytical solution is limited to high *Pe* number where the contributions of the longitudinal dispersive term are negligible and were obtained under the assumption of conservative ionic strength. We compare the analytical solution to that obtained with the numerical code RETRASO [*Saaltink et al.*, 2004], which accounts for the full dispersion tensor contribution and is not restricted by the ionic strength values.

[39] The domain simulated numerically is a rectangle, with $(x, y) = [0, 500] \times [-100, 200]$. The domain is discretized on a regular grid of 30×41 elements, having the same orientation of the flux to reduce numerical dispersion.

[40] Transport parameters are set as $V = 5.33 \times 10^{-5}$ m s^{-1}, $D_L = 3.2 \times 10^{-4}$ m^2 s^{-1}, $D_T = 1.6 \times 10^{-4}$ m^2 s^{-1}, and $n = 0.3$. The concentration of the primary species and the ionic strength of the end-members used in the simulations are listed in Table 2.

[41] It is important to highlight the assumptions underlying the present example, which may lead to some limitations when interpreting real precipitation/dissolution processes. We stress that the example is used as an illustration of the advantages of the method, and furthermore, as a way to define a potential benchmark problem for multispecies reactive transport codes. One limitation comes from noticing that dissolution and precipitation may lead to changes in medium properties [*Sanford and Konikow*, 1989; *Singurindy et al.*, 2004; *Emmanuel and Berkowitz*, 2005], specifically in porosity and groundwater velocity. While these effects may be included in RETRASO (via updating medium properties), it is complex to integrate them in the context of analytical solutions. Thus, in this example, we neglect such effects and assume that modifications in the amount of calcite only involve very thin layers of the matrix, so that no significant variations of the pore system and flow field occur. Actually, *Redden et al.* [2005] have shown that thin layers of precipitated calcite might effectively block the two interacting waters, thus preventing mixing. Their inflowing waters are subsaturated with respect to calcite. Our work (and our example) assumes perfect equilibrium at all points and at all times.

[42] Last, we used unrealistic values of the dispersion tensor components. The reason is that we wanted to enhance the impact of precipitation to better illustrate the method. This is a typical approach used in other benchmark problems such as the Henry or the Elder problems in variable density flow problems.

[43] In the first simulation, we introduce end-members (a) and (b) (Table 2) into the system at locations $y > 0$ and $y < 0$, respectively. While the former may represent fresh groundwater, the latter is a modification of a saline groundwater used by *Rezaei et al.* [2005] in a freshwater-saltwater chemical interaction problem.

[44] Controlling species in the system are $CO_{2(aq)}$, pH, and ionic strength. The latter is assumed conservative and therefore depends linearly on α. On the contrary, the two nonconservative primary species display a nonlinear behavior with α, as shown in Figure 2. Here dashed lines represent the linear behavior that would characterize a nonreactive system. The depicted analytical profiles are representative of any section transverse to flow (x = constant) because α depends solely on the normalized transverse coordinate, η [equation (20)]. Mixing-driven reactions induce an increase in pH and a reduction in c_{CO_2} when compared to the nonreactive solution. Figure 3 displays the dependence of Ca^{2+} and CO_3^{2-} on α. Now c_{Ca2+} and, to a more significant extent, $c_{CO_3^{2-}}$ values are larger than the corresponding conservative distributions. Figures 2 and 3 also compare analytical profiles with numerical RETRASO solutions at x = 450 m (that is, Pe = 150). From these figures we can deduce that mixing of end-members (a) and (b) leads to dissolution of calcite causing higher Ca^{2+} and CO_3^{2-} concentrations and higher pH, which

Table 2. Concentration of Primary Species and Ionic Strength of the End-Members Used in the Simulations[a]

End-Member	pH	C_{CO_2} (mol/kg$_{water}$)	I_s
(a)	7.3	3.40 E−4	0.005
(b)	7.16	3.51 E−4	0.625
(c)	7.3	3.40 E−4	0
(d)	7.3	3.40 E−5	0

[a]All end-members are in equilibrium with respect to calcite.

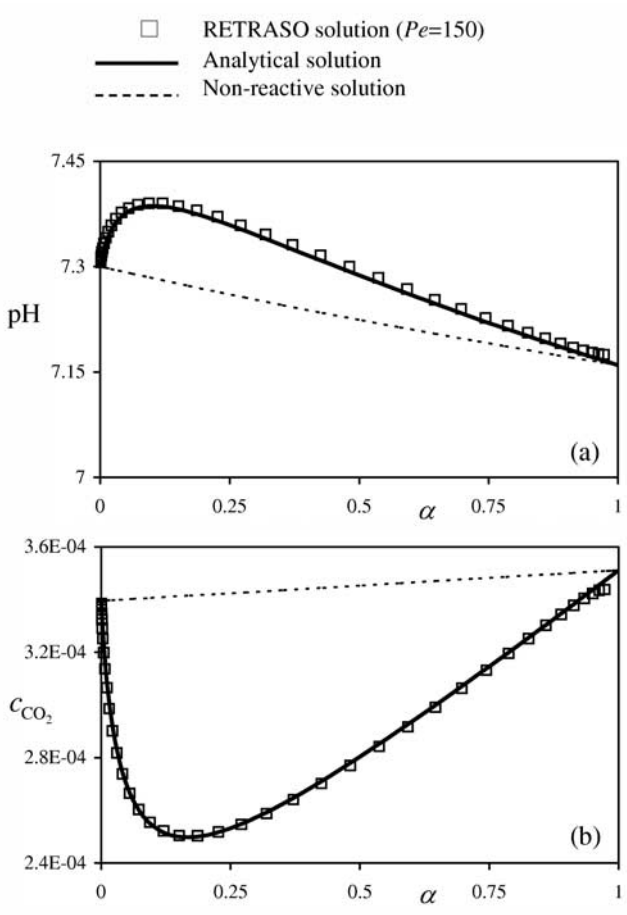

Figure 2. Dependence of pH and c_{CO_2} (mol/kg$_{water}$) on α when continuously flushing end-members (a) and (b) (Table 2) on ($x = 0$, $y > 0$) and ($x = 0$, $y < 0$), respectively. Continuum bold lines refer to analytical solutions, symbols (□) refer to RETRASO numerical results at $x = 450$ m ($Pe = 150$). Dashed lines correspond to the solution for nonreactive solutes.

in turn causes lower CO_2 concentrations. Increase in CO_3^{2-} concentrations is more important than for Ca^{2+} in relative terms (the last is indeed hardly noticeable). The reason is that CO_3^{2-} concentrations are about 3 orders of magnitude lower than those of Ca^{2+}. Calcite dissolution releases equal amounts of $Ca^{2+}$and CO_3^{2-} in absolute terms, having a greater effect on the low CO_3^{2-} concentrations in relative terms.

[45] Figures 4a and 5a contain the normalized rates, $\tilde{r}_2 = r_2 x / (nVc_0)$ and $\tilde{r}_3 = r_3 x / (nVc_0)$ (here c_0 is a reference concentration, set as unity), corresponding to one aqueous [equation (14b)] and one nonaqueous [equation (14c)] reaction (CO_3^{2-} depletion and calcite dissolution, respectively). In Figure 5a we also compare the analytical distribution of $\tilde{r}_3$ with the numerical RETRASO solution at $x = 450$ m (or $Pe = 150$). No numerical solution is presented in Figure 4a since the code does not provide aqueous reaction rates. Both $\tilde{r}_2$ and $\tilde{r}_3$ are negative. This implies that a source term is appearing in CO_3^{2-} and Ca^{2+} mass balances and calcite dissolution occurs throughout the system. We notice (Figure 5a) that the maximum dissolution occurs at low α value, where freshwater is dominant. Figure 5a also displays the calcite saturation index profile (SI = IAP / K, IAP being the ion activity product and K the equilibrium constant) for a nonreactive mixing. We notice that the predicted dissolution process is shifted toward much fresher zones than suggested by the SI profile, which is based on nonreactive mixing. This highlights that rather than SI being the most relevant factor controlling dissolution, it is in fact the interaction between transport and chemical reactions what really affects dissolution patterns. This finding is consistent with numerical results of *Rezaei et al.* [2005] and experimental evidences of *Singurindy et al.* [2004]. In Figure 4b we plot the dependence on α of the two factors, $(d\alpha / d\eta)^2$ and $\partial^2 c''_{am} / \partial\alpha^2$, which contribute to $\tilde{r}_2$. The first factor is controlled by transport features, while the second one is related to the nonlinearity in the speciation. A similar plot is provided for $\tilde{r}_3$ in Figure 5b. Figures 4b and 5b confirm that both transport and chemical processes contribute to reaction rates and show that locations of reactive zones are mostly governed by $\partial^2 c''_{am} / \partial\alpha^2$ (notice that in Figures 4b and 5b, the α axes are plotted on a logarithmic scale). In Figures 4b and 5b, on a smaller scale, we also plot the three terms that contribute to $\partial^2 c''_{am} / \partial\alpha^2$ highlighted in equation (24). Notice that these terms need not be of the same sign. It would be hard to propose general rules stating which one of the addends is the dominant one, thus highlighting that both

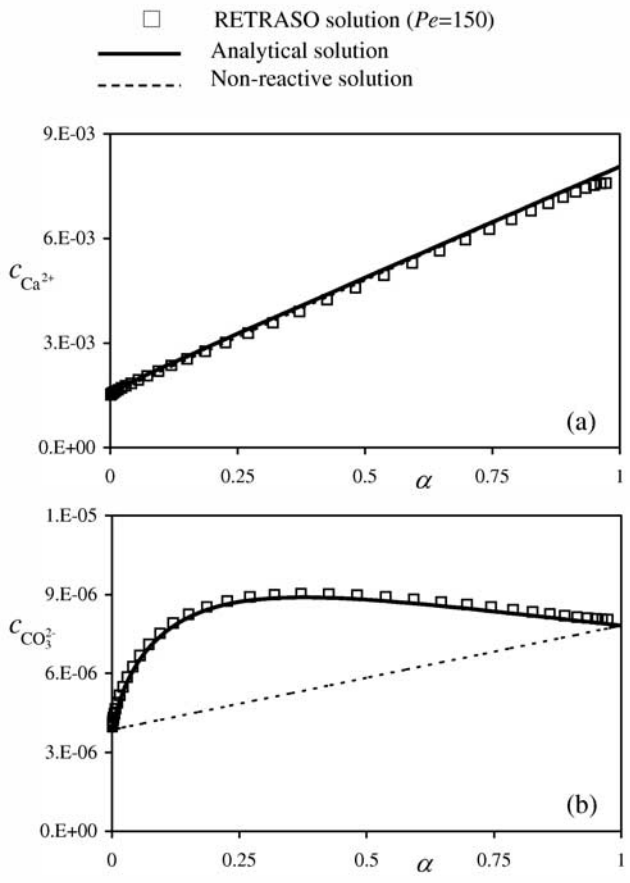

Figure 3. Dependence of $c_{Ca^{2+}}$ and $c_{CO_3^{2-}}$ (mol/kg$_{water}$) on α (same end-members as those in Figure 2). Continuum bold lines refer to analytical solutions, symbols (□) refer to RETRASO numerical results at $x = 450$ m. Dashed lines correspond to the solution for nonreactive solutes.

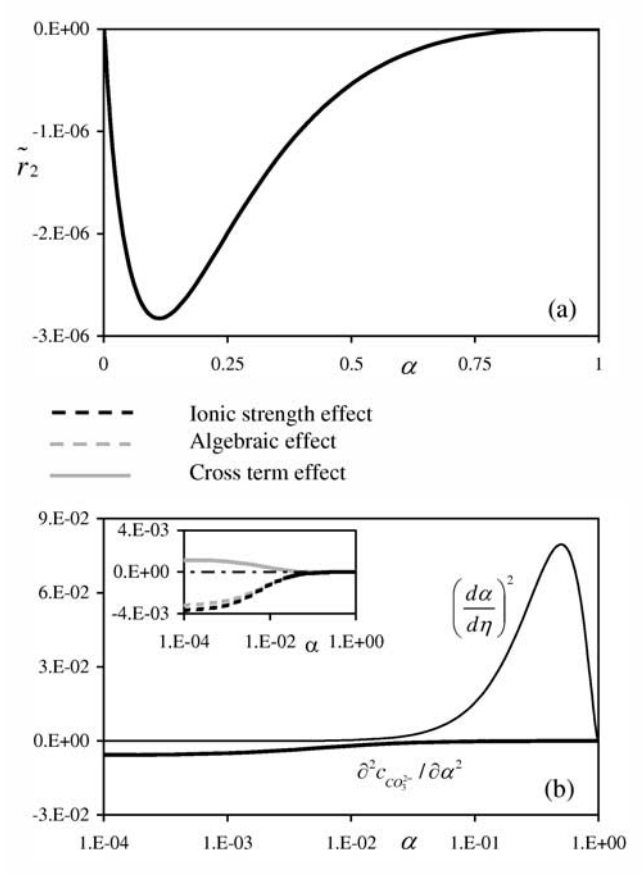

Figure 4. (a) Dependence of $\tilde{r_2}$ on α; (b) Dependence of $(d\alpha / d\eta)^2$ and $\partial^2 c_{CO_3^{2-}} / \partial \alpha^2$ on α; the insert depicts the three contributions highlighted in equation (24), the algebraic effect, the cross term effect, and the ionic strength effect (first, second, and third addend in the right-hand side of equation (24), respectively). Same end-members as those of Figure 2.

algebraic and ionic strength effects should be considered to properly evaluate reaction rates.

[46] The agreement observed in Figures 2, 3, and 5a between analytical and numerical solutions for $Pe = 150$ is quite satisfactory, thus revealing the small influence of the simplifications of negligible longitudinal dispersion and conservative ionic strength involved in the analytical solution. The minor discrepancies at values of α close to 1 are probably due to the presence of the numerical domain boundary, not incorporated in our analytical solution. Further, the slight underestimation of the (negative) peak of $\tilde{r}_3$ provided by RETRASO (Figure 5a) may be partly related to the fact that the analytical solution is valid for very large Pe numbers. Indeed, the observed discrepancy between numerical and analytical solutions tends to decrease with increasing Peclet numbers.

[47] We highlight that the analytical solution has evidenced that the functional dependences of the variables of interest can be synthesized using the single similarity variable η (or α) thus allowing depicting the behavior of each variable in a single one-dimensional plot (i.e., Figure 5a). To better exemplify the two-dimensional pattern of dissolution inside the system and demonstrate the capability of the proposed analytical solution to simulate calcite dissolution through the whole domain (and thus also in that part where Pe is small), Figure 6 depicts the iso-lines of r_3 obtained analytically (continuum lines) and by using RETRASO (dashed lines).

[48] It clearly emerges that dissolution tends to develop inside the fresher part of the domain and is mostly concentrated near the end-members entrance side.

[49] We notice that analytical results perfectly agree with the numerical r_3 distribution even at locations close to the end-members entrance side. Some discrepancies appear along the direction of maximum longitudinal development of the dissolution pattern, because of the approximation of neglecting longitudinal dispersive contributions in the analytical results.

[50] In a mixing problem within the carbonate system, the presence of precipitation or dissolution of calcite depends on the composition of the end-members. The nonlinearity of the process makes it difficult to predict the system behavior (without fully solving the problem). As an example, we simulate the mixing of end-members (c) and (d) of Table 2

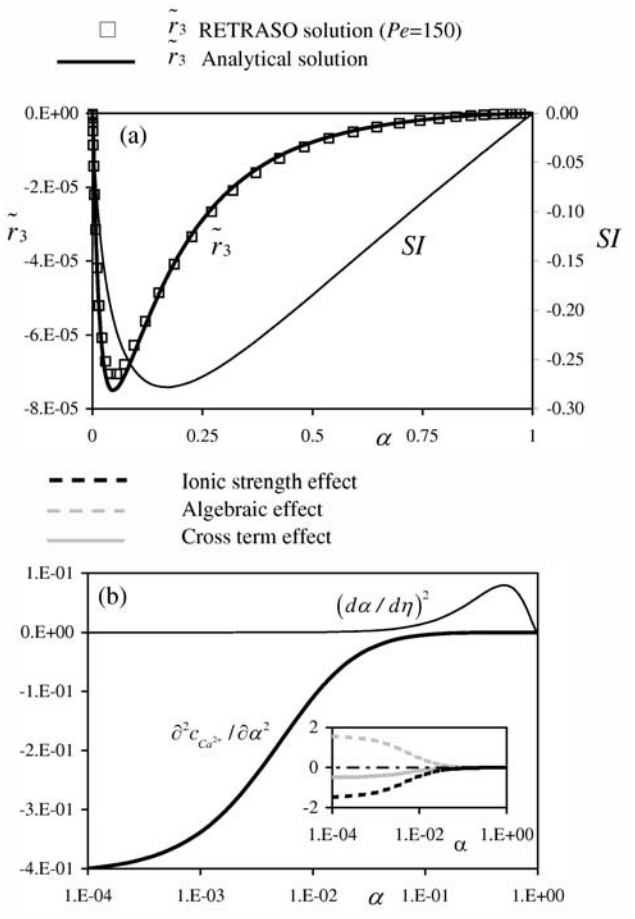

Figure 5. (a) Dependence on α of saturation index (SI) and $\tilde{r_3}$, continuum bold lines refer to analytical $\tilde{r_3}$ and symbols (□) refer to RETRASO numerical $\tilde{r_3}$ at $x = 450$ m; (b) Dependence of $(d\alpha / d\eta)^2$ and $\partial^2 c_{CO_3^{2-}} / \partial \alpha^2$ on α; the insert depicts the three contributions highlighted in equation (24), the algebraic effect, the cross term effect, and the ionic strength effect (first, second, and third addend in the right-hand side of equation (24), respectively). Same end-members as those of Figure 2.

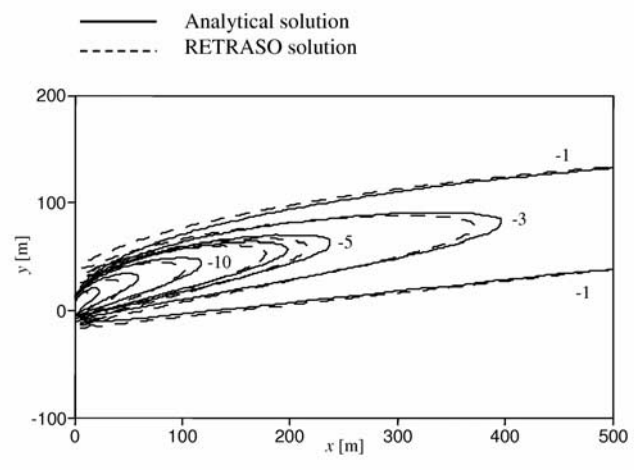

Figure 6. Iso-lines of r_3 (10^{-9} mol m^{-3} s^{-1}); continuum lines refer to analytical results, dashed ones refer to RETRASO numerical results. Same end-members as those of Figure 2.

in the same setup displayed in Figure 1a. Figure 7 depicts the dependence of $\tilde{r}_3$ on α for this problem, comparing analytical and numerical solutions. In this configuration we find precipitation on one side (water with higher CO_2 content) and dissolution on the other side.

5. Summary and Discussion

[51] We propose a novel mixing ratios-based formulation to evaluate solute concentrations and reaction rates when equilibrium aqueous reactions and precipitation/dissolution of minerals are driven by the mixing of different end-members. The methodology comprises the following four major steps: (1) solving the conservative transport equations satisfied by mixing ratios; (2) defining and evaluating the conservative components of the system; (3) performing speciation calculations; and (4) evaluating reaction rates.

[52] Our main result is encapsulated in a general and concise expression for reaction rates [equation (13)] that demonstrates that the amount of reactants evolving into products depends on the rate at which the end-members mix, which is in turn controlled by the dispersive processes [*Cirpka et al.*, 1999; *Nambi et al.*, 2003; *Chu et al.*, 2005; *Knutson et al.*, 2005; *Emmanuel and Berkowitz*, 2005]. The term $\nabla^T \alpha_i \mathbf{D} \nabla \alpha_i$ in equation (13) depends solely on flow and transport parameters and can be used as a measure of the mixing rate. This is consistent with the ideas underlying the concept of dilution index, as defined by *Kitanidis* [1994].

[53] The general expression derived for reaction rates may be used to estimate the dispersive properties of the system once solute concentrations, mixing ratios, and reaction rates are known. In this sense, equation (13) could be used as an alternative to classical (reactive or conservative) tracer tests to estimate the dispersion tensor components. A very similar concept was recently proposed by *Cirpka et al.* [2006] for the particular case of acid-base reactions.

[54] An innovation of the proposed methodology with respect to previous work [*Lichtner*, 1985; *Steefel and Mac Quarrie*, 1996; *Saaltink et al.*, 1998; *Molins et al.*, 2004; *De Simoni et al.*, 2005] consists in reformulating the reactive transport problem in terms of proportions of mixing (i.e., mixing ratios). The attractiveness of this approach is that the solution is then achieved by solving individual transport equations for as many mixing ratios as the number of end-members, *Ni*, minus one. This feature may result in computational savings when $Ni - 1$ is smaller than the number of components needed to fully define the chemical system (in our example of section 4, these components were two). Another advantage of the proposed approach is that it may allow deriving novel analytical solutions for reactive transport problems whenever analytical solutions are known for the transport equations of conservative quantities (i.e., for simple geometries, flow and transport configurations). These solutions can be used, for instance, as benchmark problems for testing numerical codes or in designing/interpreting experimental analyses devoted to study mixing-driven reactive transport processes.

[55] In many practical problems, some species (such as minerals) may appear (in response to the changes caused by reactions) or disappear (by being totally dissolved) within regions of the domain. This feature can be handled within the context of our methodology by defining different chemical systems for each zone, to solve separately. This would lead to an increased computational burden because of the need to update the chemical system wherever and whenever new species appear or disappear. As an example, if no mineral is present at a point, it is impossible to guarantee chemical equilibrium at that particular point, and transport becomes, in practice, conservative for all aqueous species.

[56] To illustrate potential applications and usefulness of the proposed formulation, we solve the pseudo-stationary mixing of two different $CaCO_3$-saturated solutions in a two-dimensional setup in the presence of uniform flow. Our methodology clearly demonstrates that the mixing-driven calcite dissolution/precipitation may be formulated in terms of a single conservative component, the mixing ratio. This offers an explanation of the capability of the method developed by *Sanford and Konikow* [1989] to model calcite dissolution in the fresh-salt water mixing zone by trans-

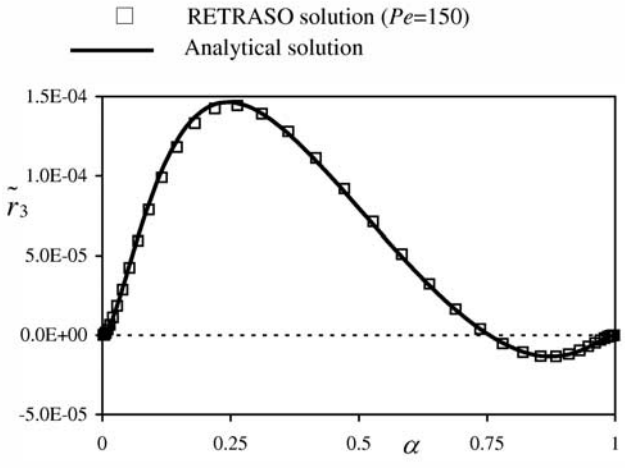

Figure 7. Dependence of $\tilde{r}_3$ on mixing ratio α when flushing end-members (c) and (d) (Table 2) on ($x = 0$, $y > 0$) and ($x = 0$, $y < 0$), respectively. Continuum bold lines refer to analytical solutions and symbols (□) refer to RETRASO numerical results at $x = 450$ m. Dashed line corresponds to $\tilde{r}_3 = 0$.

porting a single component, while, according to classical components-based formulations, two components are needed to fully define the system.

[57] The results we obtained in simulating calcite precipitation/dissolution in the saltwater mixing zone of coastal aquifers properly reproduce the nonlinear behavior of the process with modest computational efforts in comparison to multicomponent reactive transport numerical codes. Our solution is thus proposed as a promising tool to investigate the evolution of carbonate systems.

[58] **Acknowledgments.** The second, third, and fourth authors acknowledge financial support by Enresa and the European Union through projects FUNMIG and GABARDINE. We would like to thank Alberto Guadagnini for his useful suggestions in the preparation of this paper.

References

Andre, B. J., and H. Rajaram (2005), Dissolution of limestone fractures by cooling waters: Early development of hypogene karst systems, *Water Resour. Res.*, *41*, W01015, doi:10.1029/2004WR003331.

Aucour, A. M., F. A. Tao, P. Moreira-Turcq, P. Seyler, S. Sheppard, and M. F. Benedetti (2003), The Amazon River: behaviour of metals (Fe, Al, Mn) and dissolved organic matter in the initial mixing at the Rio Negro/Solimoes confluence, *Chem. Geol.*, *197*, 271–285.

Balistrieri, L. S., S. E. Box, and J. W. Tonkin (2003), Modelling precipitation and sorption of elements during mixing of river water and porewater in the Couer d'Alene River basin, *Environ. Sci. Technol.*, *37*, 4694–4701.

Carrera, J., E. Vázquez-Suñé, O. Castillo, and X. Sanchez-Vila (2004), A methodology to compute mixing ratios with uncertain end-members, *Water Resour. Res.*, *40*, W12101, doi:10.1029/2003WR002263.

Choi, J., S. M. Hulseapple, M. H. Conklin, and J. W. Harvey (1998), Modeling CO2 degassing and pH in a stream-aquifer system, *J. Hydrol.*, *209,* 297–310.

Chu, M., P. K. Kitanidis, and P. L. McCarty (2005), Modeling microbial reactions at the plume fringe subject to transverse mixing in porous media: When can the rates of microbial reaction be assumed to be instantaneous?, *Water Resour. Res.*, *41*, W06002, doi:10.1029/2004WR003495.

Cirpka, O. A., E. O. Frind, and R. Helmig (1999), Numerical simulation of biodegradation controlled by transverse mixing, *J. Contam. Hydrol.*, *40*, 159–182.

Cirpka, O., A. Olsson, Q. Ju, M. A. Rahman, and P. Grathwohl (2006), Determination of transverse dispersion coefficients from reactive plume lengths, *Ground Water*, *44*, 212–221.

Corbella, M., C. Ayora, and E. Cardellach (2003), Dissolution of deep carbonate rocks by fluid mixing: A discussion based on reactive transport modelling, *J. Geochem. Explor.*, *78-9*, 211–214.

De Simoni, M., J. Carrera, X. Sanchez-Vila, and A. Guadagnini (2005), A procedure for the solution of multi-component reactive transport problems, *Water Resour. Res.*, *41*, W11410, doi:10.1029/2005WR004056.

Emmanuel, S., and B. Berkowitz (2005), Mixing-induced precipitation and porosity evolution in porous media, *Adv. Water Resour.*, *28*, 337–344.

Gabrovšek, F., and W. Dreybrodt (2000), Role of mixing corrosion in calcite-aggressive H_2O-CO_2-$CaCO_3$ solutions in the early evolution of karst aquifers in limestone, *Water Resour. Res.*, *36*, 1179–1188.

Gramling, C., C. F. Harvey, and L. C. Meigs (2002), Reactive transport in porous media: A comparison of model prediction with laboratory visualization, *Environ. Sci. Technol.*, *36*, 2508–2514.

Haberman, R. (1998), Elementary applied partial differential equations, Prentice-Hall, Upple Saddle River, N. J.

Helgerson, H. C., and D. H. Kirkham (1974), Theoretical prediction of the thermodynamic behaviour of aqueous electrolytes at high pressure and temperature: II Debye-Hückel parameters for activity coefficients and relative partial molo properties, *Am. J. Sci.*, *274*, 1199–1261.

Jose, S. C., and O. A. Cirpka (2004), Measurement of mixing-controlled reactive transport in homogeneous porous media and its prediction from conservative tracer test data, *Environ. Sci. Technol.*, *38*, 2089–2096.

Kaufmann, G. (2003), Numerical models for mixing corrosion in natural and artificial karst environments, *Water Resour. Res.*, *39*(6), 1157, doi:10.1029/2002WR001707.

Kitanidis, P. K. (1994), The concept of the dilution index, *Water Resour. Res.*, *30*, 2011–2026.

Knutson, C. E., C. J. Werth, and A. J. Valocchi (2005), Pore-scale simulation of biomass growth along the transverse mixing zone of a model two-dimensional porous medium, *Water Resour. Res.*, *41*, W07007, doi:10.1029/2004WR003459.

Lichtner, P. C. (1985), Continuum model for simultaneous chemical reactions and mass transport in hydrothermal systems, *Geochim. Cosmochim. Acta*, *49*, 779–800.

Molins, S., J. Carrera, C. Ayora, and M. W. Saaltink (2004), A formulation for decoupling components in reactive transport problems, *Water Resour. Res.*, *40*, W10301, doi:10.1029/2003WR002970.

Nambi, I., C. Werth, R. Sanford, and A. Valocchi (2003), Pore-scale analysis of anaerobic halorespiring bacterial growth along the transverse mixing zone of an etched silicon pore network, *Environ. Sci. Technol.*, *37*, 5617–5624.

Parkhurst, D. L. (1995), User's guide to PHREEQC—A compute program for speciation, reaction-path, advective-transport, and inverse geochemical calculations. *U.S. Geological Survey Water-Resources Investigations Report*, Lakewood, CO.

Redden, G. D., Y. Fang, T. Scheibe, A. Tartakovsky, D. T. Fox, T. A. White, Y. Fujita, and M. E. Delwiche (2005), Calcium carbonate precipitation along solution-solution interfaces in porous media, *Eos Trans. AGU*, *86*(52), Fall Meeting Supplement, Abstract B33C-1042.

Rezaei, M., E. Sanz, E. Raeisi, E. Vázquez-Suñé, C. Ayora, and J. Carrera (2005), Reactive transport modeling of calcite dissolution in the salt water mixing zone, *J. Hydrol.*, *311*, 282–298.

Romanov, D., and W. Dreybrodt (2006), Evolution of porosity in the saltwater-freshwater mixing zone of coastal carbonate aquifers: An alternative modelling approach, *J. Hydrol.*, *329*(3–4), 661–673.

Rueedi, J., R. Purtschert, U. Beyerle, C. Alberich, and R. Kipfer (2005), Estimating groundwater mixing ratios and their uncertainties using a statistical multi parameter approach, *J. Hydrol.*, *305*, 1–14.

Saaltink, M. W., C. Ayora, and J. Carrera (1998), A mathematical formulation for reactive transport that eliminates mineral concentrations, *Water Resour. Res.*, *34*, 1649–1656.

Saaltink, M. W., F. Batlle, C. Ayora, J. Carrera, and S. Olivella (2004), RETRASO, a code for modeling reactive transport in saturated and unsaturated porous media, *Geol. Acta*, *2*, 235–251.

Sanford, W. E., and L. F. Konikow (1989), Simulation of calcite dissolution and porosity changes in saltwater mixing zones in coastal aquifers, *Water Resour. Res.*, *25*, 655–667.

Singurindy, O., B. Berkowitz, and R. P. Lowell (2004), Carbonate dissolution and precipitation in coastal environments: Laboratory analysis and theoretical consideration, *Water Resour. Res.*, *40*, W04401, doi:10.1029/2003WR002651.

Steefel, C. I., and K. T. B. Mac Quarrie (1996), Approaches to modelling reactive transport, *Reactive transport in porous media, Rev. Mineral*, *34*, 83–129, Mineral. Soc. Am., Washington, D.C.

Tonkin, J. W., L. S. Balistrieri, and J. W. Murray (2002), Modeling metal removal onto natural particles formed during mixing of acid rock drainage with ambient surface water, *Environ. Sci. Technol.*, *36*, 484–492.

Witters, H. E. (1998), Chemical speciation dynamics and toxicity assessment in aquatic systems, *Ecotoxicol. Environ. Saf.*, *41*, 90–95.

J. Carrera, Institut de Ciències de la Terra Jaume Almera, CSIC, C/Lluís Solé i Sabarís s/n, 08028 Barcelona, Spain.

M. De Simoni, Dipartimento di Ingegneria Idraulica, Ambientale, Infrastrutture Viarie, Rilevamento, Politecnico di Milano, Piazza L. Da Vinci 32, 20133 Milano, Italy.

M. W. Saaltink and X. Sanchez-Vila, Department of Geotechnical Engineering and Geosciences, Technical University of Catalonia, C/Jordi Girona 1-3, 08034 Barcelona, Spain. (xavier.sanchez-vila@upc.edu)